A Compact Microstrip Lowpass Filter with Flat Group-delay and Ultra High Figure-of-Merit

M. Hayati [1,2], M. Ekhteraei [1], and F. Shama [1]

[1] Electrical Engineering Department
Kermanshah Branch, Islamic Azad University, Kermanshah, Iran
Mohsen_hayati@yahoo.com, m.ekhteraei.ir@ieee.org, f.shama@aut.ac.ir

[2] Electrical Engineering Department
Razi University, Tagh-E-Bostan, Kermanshah-67149, Iran

Abstract ─ This paper presents a new design of a microwave low pass filter (LPF) using coupled stepped impedance patches. The designed LPF has specifications such as ultra sharp roll-off, ultra wide stopband, low insertion-loss and high return-loss in the passband. The designed LPF has -3 dB cut-off frequency of 1.38 GHz. The transition-band is 0.12 GHz that is from 1.38 to 1.50 GHz with the attenuation levels of -3 and -20 dB, respectively. Maximum insertion-loss at about 80% of the passband is 0.1 dB. The simulation and experimental results are close to each other. The proposed LPF achieved to a remarkable figure-of-merit of 171622.

Index Terms ─ Bended structure, group delay, lowpass filter, microstrip.

I. INTRODUCTION

Within the development of modern communication technologies, demands for pure signals are increasing rapidly. So, in order to get pure signals, high performance LPFs have been widely used. Recently, many microstrip LPFs are realized by various structures. In [1], a structure consists of high-impedance meandered transmission lines loaded by triangular and polygonal resonant patches is presented. Although the filter has wide stopband but it has a low return-loss in the passband. An LPF consists of radial resonators is presented in [2]. The structure has a sharp roll-off and compact size but the stopband is not so wide. Dual-transmission line is suggested to design an LPF in [3]. The filter has sharp roll-off and high return-loss in the passband, but it has also poor specifications such as very large size and narrow stopband width. In [4], an LPF employs rat-race directional couplers properly arranged to operate as bandstop transversal filtering sections (TFSs) is presented, which has a sharp roll-off but also suffers from a large size. A compact LPF using a T-shaped patch and stepped impedance resonators with sharp roll-off is presented in [5]. But the value of return-loss in the passband is not high. An LPF structure which consists of a high impedance microstrip line (HIML) and a pair of radial stubs (RSs) loaded at its center and a pair of stepped impedance open stubs (SIOSs) loaded on both ends of HIML, is designed in [6]. Despite having a wide stopband and high return-loss, it has poor characteristics such as large size and gradual cut-off. In this paper, a compact microstrip lowpass filter using coupled stepped impedance patches with ultra wide stopband, remarkable roll-off rate and noticeable figure-of-merit (FOM) of 171,622 is designed.

II. DESIGN PROCEDURE

At the first step, the resonator is analyzed and the process of designing the resonator is represented step by step; at the second step, the suppressor is analyzed and designed as well.

A. Design and analysis of the resonator

The main idea in the resonator design contains to have a two resonator which occupies a one resonator area (each resonator creates a one transmission zero nearby the cut-off frequency and results in a sharp roll off). This case can be occurred using the bending technique, which allows the resonators to fold in each other, which results a compact size.

1) First resonator design

The LC circuit and layout of the prototype resonator are shown in Fig. 1. Based on the basic concepts and theories of microstrip filters, a short open circuited stub of a lossless microstrip line can be considered as a shunt capacitor and a similar short-circuited stub can be considered as a shunt inductor. The parameters of the transmission line of the prototype resonator as well as the physical lengths of the low and high impedance lines are obtained as follows [7]:

Submitted On: August 23, 2016
Accepted On: November 27, 2016

$$l_{Li} = \frac{\lambda_{g_{Li}}}{2\pi} \sin^{-1}\left(\frac{Z_0 \times g_i}{Z_{0L_i}}\right), \quad (1)$$

$$l_{Ci} = \frac{\lambda_{g_{Ci}}}{2\pi} \sin^{-1}\left(\frac{Z_{0C_i} \times g_i}{Z_0}\right), \quad (2)$$

where Z_{0C_i} and Z_{0L_i} represent the impedance transmission lines with low and high impedance, respectively, g_i is the element value of each part of the prototype layout, $\lambda_{g_{Li}}$ and $\lambda_{g_{Ci}}$ is the guided wavelength of high and low impedance lines, respectively.

A comparison of the S-parameters of LC model and layout of the prototype resonator is shown in Fig. 1. As shown, the frequency response has a low insertion loss in the passband, but the transition band is not sharp enough. Moreover, to achieve a lower cut-off frequency, in conventional type the size should be increased, which is not desired. Therefore, to improve the performance, bending technique is employed. Bending in designing microstrip structures is a technique for reducing the size of the filters [7].

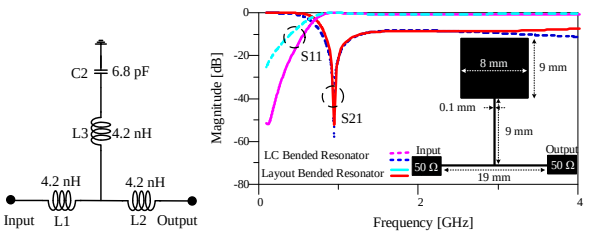

Fig. 1. The prototype resonator, the LC circuit, the layout and the simulated S-parameters.

The first bended resonator, its equivalent LC circuit and a comparison of the S-parameters of LC model and layout of the bended resonator are shown in Fig. 2 (a). In comparison with the structure shown in the Fig. 1, the size of the bended structure is more compact.

2) Second resonator design

By Similar procedure, another bended resonator is designed to have a new transmission zero nearby the previous one in first resonator; the LC model, layout of the second resonator and a comparison of the S-parameters of this resonator and its LC model are shown in Fig. 2 (b).

3) Combination of first and second resonator

With merging the first and second bended resonators, as shown in Fig. 2 (c) (with specifications of bended technique, the overall size of the resonator has not been increased), a sharper transition band can be achieved in order to have two transmission zeros nearby each other. The LC model and a comparison of the simulated S-parameters of the merged resonator and its LC model are illustrated in Fig. 2 (c). The merged resonator has two transmission zeros at 1.1 and 1.36 GHz, which creates a transition band of 0.26 GHz from -3 dB to -40 dB. But unfortunately, as highlighted in Fig. 4 (b), the insertion loss has a significant value in the passband.

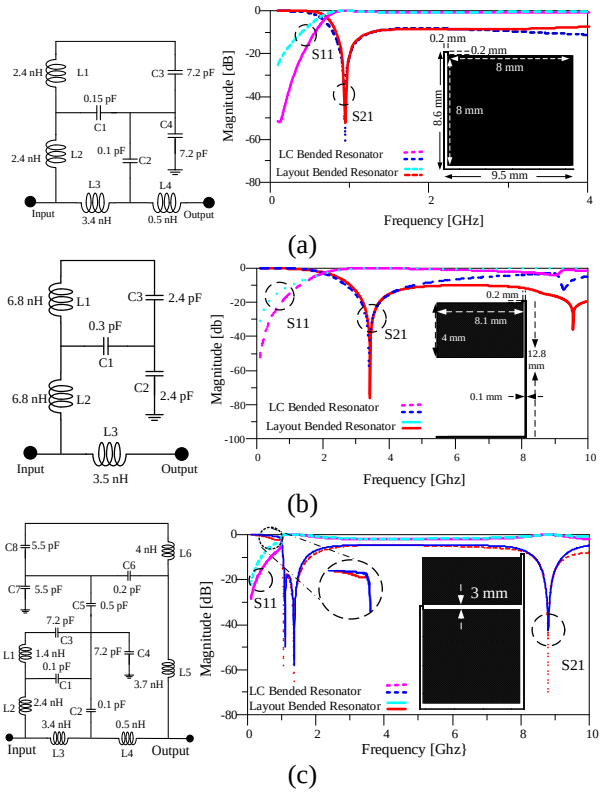

Fig. 2. The LC model, the layout and the simulated S-parameters: (a) the first bended resonator, (b) the second bended resonator, and (c) the merged resonator.

4) The proposed modified resonator

To achieve a better performance especially a low insertion loss, the structure of the merged resonator is modified by defecting the squired-shaped open stubs as shown in Fig. 3 (a). In this figure, the dimensions are indicated on this structure. The LC equivalent circuit is illustrated in Fig. 3 (b). The defection procedure not only results a better roll-off and higher return loss in the passband region, but also guarantee a small circuit area. Figure 3 (c) shows a comparison of the S-parameters of LC model and layout of the proposed modified resonator.

B. Design and analysis of the suppressor

To obtain an LPF with desired characteristics such as an ultra-wide rejection band, a modified radial patch cell (MRPC) is used as the suppressor. The LC model, layout of a prototype radial patch cell (RPC) and a comparison of the LC model and simulated S-parameters of this cell are shown in Fig. 4. As shown, this resonator cannot provide a wide rejection band, also the attenuation level is not sufficient in this region. To achieve wide rejection band and preferred attenuation level the

bending technique has been used to have a MRPC as shown in Fig. 5. The LC equivalent circuit of the MRPC and a comparison of the LC model and simulated S-parameters of MRPC are shown in Fig. 5.

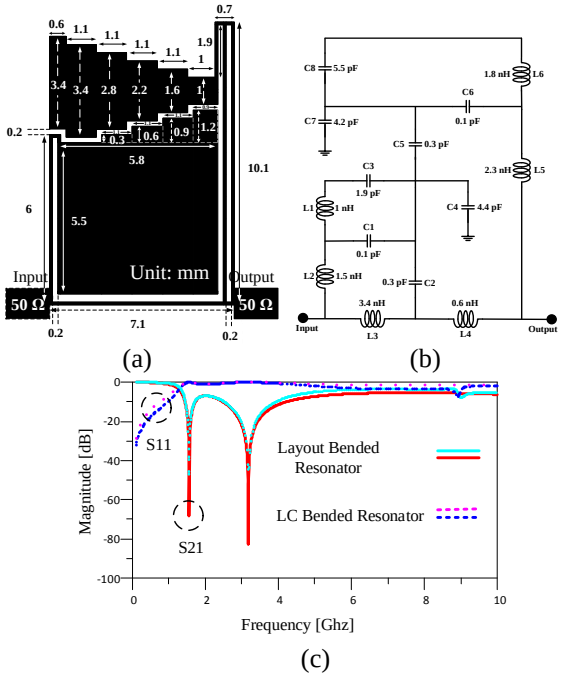

Fig. 3. The proposed modified resonator: (a) layout, (b) LC model, and (c) the simulated S-parameters.

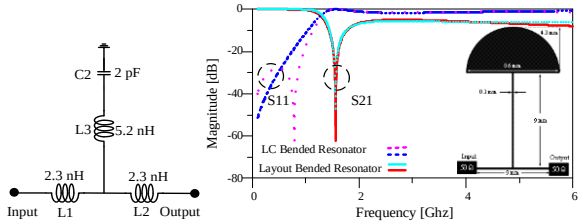

Fig. 4. A prototype RPC; the LC model, the layout and the simulated S-parameters.

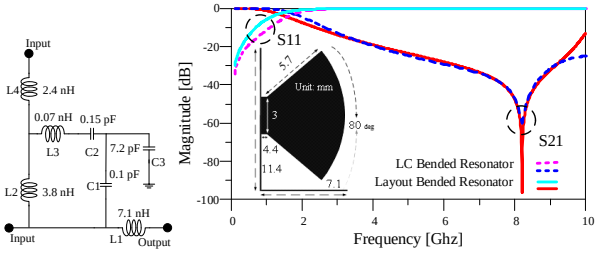

Fig. 5. A MRPC; the LC model, the layout and the simulated S-parameters.

As seen from this figure, the simulated S-parameters of this suppressor results in a wide stopband (4.2 to 9.7 GHz, with corresponding attenuation level of -20 dB), which is created by a transmission zero at 8.2 GHz with attenuation level of -96 dB. Also, the proposed MRPC occupies a smaller area than the conventional RPC.

III. LPF DESIGN

Merging the proposed modified resonator and MRPC, results in a primal LPF before loading a triangle-shaped microwave cell, which is shown in Fig. 6. From the simulated frequency response as illustrated in this figure, the filter has a very sharp transition band and wide stopband from 1.50 to 10 GHz with corresponding attenuation level of -20 dB, but the insertion loss in the passband is not low enough. Also, a wider rejection band is desired to have an ultra-wide stopband. So, by using the free spaces between the feeding lines and the radial open stub in the proposed MRPC, two stubs can be loaded to have a high performance LPF and without size increment.

Firstly, as indicated in Fig. 6, the free space between feeding lines and the upper side of MRPC is loaded by a triangle-shaped microstrip cell. As considered from this figure stopband region is dramatically suppressed from 1.50 to 18.8 GHz with corresponding attenuation level of -20 dB. Finally, the proposed LPF can be obtained as indicated in Fig. 7, which the free space below the MRPC has been loaded by a tapered microstrip cell.

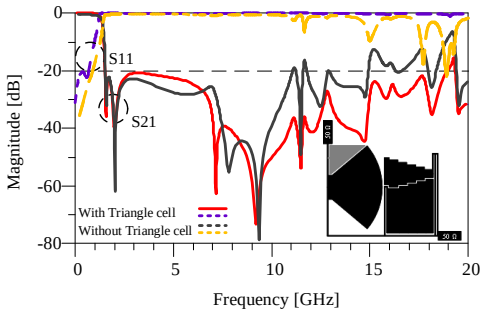

Fig. 6. Comparison between the simulated S-parameters of the layout and the triangle-shaped microwave cell before and after loading.

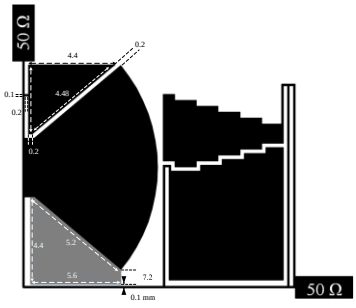

Fig. 7. The proposed LPF and the dimensions of triangle-shaped and tapered microstrip cell.

The dimensions of the loaded triangle-shaped and tapered microstrip cells to the proposed MRPC are shown in this figure.

IV. SIMULATION AND MEASUREMENT

The simulations are performed by ADS software and the measurements are carried out by an HP8757 Network Analyzer as shown in Fig. 8. As seen in Fig. 8, the final proposed filter is fabricated on the RT/Duriod 5880 substrate ($\varepsilon_r = 2.2$, thickness = 15 mil, loss tangent of 0.0009). As concluded from the final measurements, the LPF has -3 dB cut-off frequency at 1.38 GHz. The transition band is only 0.12 GHz. Maximum insertion loss is less than 0.08 dB in 78% and less than 0.2 dB in the 82% of the passband region. It has an ultra-wide stopband from 1.38 to 22.5 GHz with the attenuation level of -20 dB. The performance comparison of the proposed LPF within other published LPFs is summarized in Table 1. In this Table, the ξ is roll-off rate. RSB is the relative stop bandwidth and SF is the considered suppressing factor for the stopband. NCS is the normalized circuit size. AF is the architecture factor. Finally, FOM is the figure-of-merit for a LPF. All of these factors are defined in appendix section. As seen in Table 1, the proposed LPF has the highest FOM (171,622) among the referred LPFs.

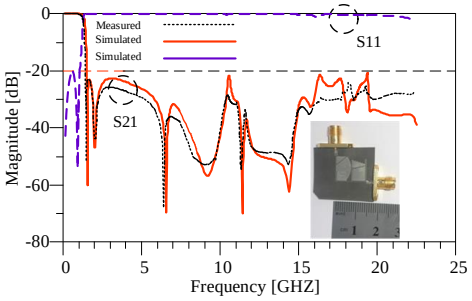

Fig. 8. The Simulated and measured S-parameters of the final proposed LPF and photograph of the proposed LPF.

A flat group delay for an LPF is desirable in the passband region [7]. As seen in Fig. 9, the maximum variation of the measured group delay in the passband is a dispensable value of 0.212 ns. The measured group delay can be determined using cure fitting as exponential functions as shown in Fig. 9. So the group delay equation can be written as bellows:

$$Group\ delay\ (s) = ae^{bf} + ce^{df}. \quad (3)$$

The group delay is considered using below equation:

$$Group\ delay\ (s) = -\frac{d\varphi}{d\omega}, \quad (4)$$

where φ is the total phase shift in radians (in this case from the parameter of S21), and ω is the angular frequency in radians per unit time, equal to $2\pi f$, where f is the frequency in hertz. From Equations (1-2) and with considering $= 2\pi f$:

$$-\frac{1}{2\pi}\frac{d\varphi}{df} = ae^{bf} + ce^{df}, \quad (5)$$

$$\int d\varphi = -2\pi \int_{0.1GHz}^{1GHz} (ae^{bf} + ce^{df})df, \quad (6)$$

$$\varphi(S_{21})|_{0.1GHz}^{1GHz} = -2\pi\left({}^{a}/_{b}\, e^{bf} + {}^{c}/_{d}\, e^{df}\right). \quad (7)$$

As shown in Fig. 10, the calculated phase of S21 parameter is illustrated in comparison with the simulated one using ADS software. As seen, it is good agreement between the measurements and simulations in this case.

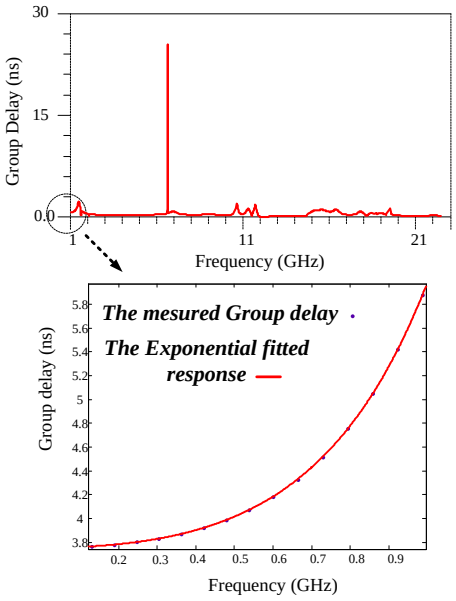

Fig. 9. The group delay in the passband for the proposed LPF.

Table 1: Comparison between the characteristics of the proposed LPF and other similar types

Ref.	f_c (GHz)	ζ	NCS	RSB	R-L (dB)	SF	AF	FOM
[1]	2.44	178.9	0.0232	1.73	12	2	1	26912
[2]	4.24	130.7	0.014	1.26	20	2	1	23526
[5]	4	425	0.0551	1.30	15.2	2	1	78928
[6]	1.07	56.67	0.0089	1.70	20	2	1	21649
[7]	1.11	58.62	0.0088	1.54	18.2	2	1	20495
[8]	1.5	81	0.017	1.72	20	2	1	16400
[9]	3.2	5.28	0.0075	1.66	16	2	1	1160
[10]	0.85	18	0.0072	1.73	17	1.5	1	6479
[11]	2	43.9	0.015	1.63	10	1	1	4771
[12]	2.4	92.5	0.037	1.35	11	3	1	10106
[13]	1.67	21.2	0.0064	1.49	12	1	1	4936
[14]	1.65	57.8	0.012	1.61	12	3.5	1	27142
[15]	1.18	36.3	0.0061	1.32	32	1.5	1	11543
[16]	3.6	370	0.01496	0.98	16	2	1	49672
This Work	1.38	324.25	0.0058	1.74	20	2	1	171622

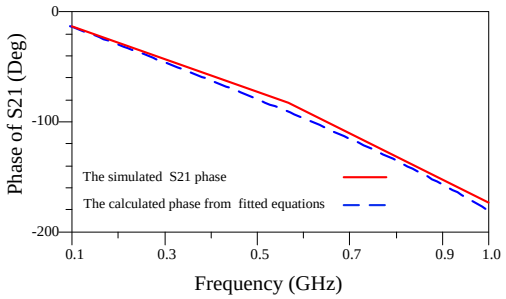

Fig. 10. The phase of S21 parameter.

V. CONCLUSION

A microstrip LPF with sharp transition band and ultra-wide stopband has been presented. By applying bended structures, without increasing the size, the cut-off frequency has been decreased. The filter passes frequencies through L-band range and highly suppresses in the higher ranges. The fabricated LPF with flat group delay in the passband can be expected to use in microwave circuits for suppressing the unwanted harmonics and signals.

ACKNOWLEDGEMENT

The authors would like to thank the Kermanshah Branch, Islamic Azad University for the financial support of this research project.

APPENDIX

In Table 1, the roll of rate (ζ) is used to evaluate the sharpness which is defined as [7]:

$$\zeta = \frac{\alpha\, max - \alpha min}{f_s - f_c} \quad (dB/GHz), \tag{8}$$

where α_{max} is the 20 (or 40 dB) attenuation point, α_{min} is the 3 dB attenuation point; f_s is the 20 dB stopband frequency; and f_c is the 3 dB cut-off frequency. The relative stopband bandwidth (RSB) is given by [7]:

$$RSB = \frac{stopbband\ bandwidth}{stopband\ center\ frequency}. \tag{9}$$

The suppression factor (SF) is based on the stopband suppression. A higher suppression degree in the stopband leads to a greater SF. For instance, if the stopband bandwidth is calculated under 20 dB restriction, then the SF is considered as 2. The normalized circuit size (NCS) is given by [7]:

$$NCS = \frac{phisical\ size\ (length*Width)}{\lambda_{g^2}}. \tag{10}$$

This is applied to measure the degree of miniaturization of diverse filters, where λ_g is the guided wavelength at 3 dB cut-off frequency, the architecture factor (AF) can be recognized as the circuit complexity factor which is signed as 1 when the design is 2D and 2 when the design is 3D. Finally, the figure of merit (FOM) is defined as [7]:

$$FOM = \frac{\zeta * RSB * SF}{NCS * AF}. \tag{11}$$

REFERENCES

[1] M. Hayati and A. Abdipour, "Compact microstrip lowpass filter with sharp roll-off and ultra-wide stopband," *Electronics Letters*, vol. 49, no. 18, pp. 1159-1160, Aug. 2013.

[2] M. Hayati, S. Naderi, and F. Jafari, "Compact microstrip lowpass filter with sharp roll-off using radial resonator," *Electronics Letters*, vol. 50, no. 10, pp. 761-2, May 2014.

[3] V. K. Velidi and S. Sanyal, "Dual-transmission-line microstrip equiripple lowpass filter with sharp roll-off," *ETRI Journal*, vol. 33, no. 6, pp. 985-8, Dec. 2011.

[4] G. R. Gómez, M. A. Sánchez-Soriano, M. Sánchez-Renedo, G, Torregrosa-Penalva and E. Bronchalo, "Extended-stopband microstrip lowpass filter using rat-race directional couplers," *Electronics Letters*, vol. 49, no. 4, pp. 272-4, Feb. 2013.

[5] M. Hayati and A. Sheikhi, "Microstrip lowpass filter with very sharp transition band using T-shaped, patch, and stepped impedance resonators," *ETRI Journal*, vol. 35, no. 3, pp. 538-41, June 2013.

[6] J. Xu, Y. X. Ji, W. Wu, and C. Miao, "Design of miniaturized microstrip LPF and wideband BPF with ultra-wide stopband," *IEEE Microwave and Wireless Components Letters*, vol. 23, no. 8, pp. 397-9, Aug. 2013.

[7] M. Hayati, F. Shama, and H. Abbasi, "Compact microstrip lowpass filter with wide stopband and sharp roll-off using tapered resonator," *International Journal of Electronics*, vol. 100, no. 12, pp. 1751-9, Dec. 2013.

[8] M. Hayati, H. Abbasi, and F. Shama, "Microstrip lowpass filter with ultrawide stopband and sharp roll-off," *Arabian Journal for Science and Engineering*, vol. 39, no. 8 pp. 6249-53, Aug. 2014.

[9] K. Ma, K. S. Yeo, and W. M. Lim, "Ultra-wide rejection band lowpass cell," *Electronics Letters*, vol. 48, no. 2, pp. 99-100, Jan. 2012.

[10] J. Wang, H. Cui, and G. Zhang, "Design of compact microstrip lowpass filter with ultra-wide stopband," *Electronics Letters*, vol. 48, no. 14, pp. 854-6, July 2012.

[11] F. Wei, L. Chen, and X. W. Shi, "Compact lowpass filter based on coupled-line hairpin unit," *Electronics Letters*, vol. 48, no. 7, pp. 379-381, Mar. 2012.

[12] J. L. Li, S. W. Qu, and Q. Xue, "Compact microstrip lowpass filter with sharp roll-off and wide stop-band," *Electronics Letters*, vol. 45, no. 2, pp. 110-1, Jan. 2009.

[13] X. B. Wei, P. Wang, M. Q. Liu, and Y. Shi, "Compact wide-stopband lowpass filter using stepped impedance hairpin resonator with radial

stubs," *Electronics Letters*, vol. 47, no. 15, July 2011.
[14] B. Zhang, S. Li, and J. Huang, "Compact lowpass filter with wide stopband using coupled rhombic stubs," *Electronics Letters*, vol. 51, no. 3, pp. 264-6, Jan. 2015.
[15] J. Wang, L. Xu, J. S. Zhao, Y. X. Guo, and W. Wu, "Compact quasi-elliptic microstrip lowpass filter with wide stopband," *Electronics Letters*, vol. 46, no. 20, pp. 1384-1385, Jan. 2015.
[16] M. Hayati, S. Roshani, S. Roshani, and F. Shama, "A novel miniaturized Wilkinson power divider with n th harmonic suppression," *Journal of Electromagnetic Waves and Applications*, vol. 27, no. 6, pp. 726-735, Apr. 2013.

Mohsen Hayati is currently a Professor in Electrical Engineering Department, Razi University, Kermanshah, Iran. He has authored or co-authored over 185 papers published in international, domestic journals and conference proceedings. His current research interests include microwave and millimeter-wave devices and circuits, application of computational intelligence, artificial neural networks, fuzzy systems, neuro fuzzy systems, electronic circuit synthesis, and modeling and simulations.

Milad Ekhteraei is currently working toward the Ph.D. degree in Electrical Engineering in Azad University, Kermanshah, Iran. His research interests include design and analysis of the microstrip filters, and antennas.

Farzin Shama is currently a Assistant Professor in the Electrical Engineering Department, Azad University, Kermanshah Branch, Iran. His research interests include the microwave engineering, passive and active circuits design. He has published more than 40 papers in international and domestic journals and conferences. He was proud to achieve Superior Researcher in the Engineering Faculty of Razi University, in 2011 and 2012. He has been selected as Top Student of Iran, awarded by First Vice President of Iran in 2015.